STUDIES OF THE EFFECT OF DEPTH OF FOCUS
ON SEISMIC PULSES

B. F. Howell, Jr.   (814-865-6821)
P. M. Lavin   (814-865-2622)

The Pennsylvania State University
Department of Geology and Geophysics
205-209 Mineral Sciences Building
University Park, Pennsylvania

Annual Report for 1965

Covering work done up to December 31, 1965

Prepared

for

STUDIES OF THE EFFECT OF
DEPTH OF FOCUS ON SEISMIC PULSES

I. Objectives

The principal objective of this research is to improve the accuracy of focal-depth determination as a means of distinguishing between natural earthquakes and explosions. The research has consisted mainly of evaluating a method of focal-depth determination which depends on recognition of the sequence of events which arise from the reflection of the initial P pulse at the surface, and evaluating the factors controlling the accuracy of this measurement.

A second objective is to study the effect of the nature of a boundary on seismic pulses refracted along it both in scale models and in the real earth.

II. Technical Status and Major Accomplishment.

A. Evaluation of the Watson-Merdler method of focal-depth determination

An earlier technical report (AFCRL-64-755) described the Watson-Merdler method of focal-depth determination in detail. A summary of this is in press in a VESIAC conference report. In brief, the method assumes that the seismogram consists of the sum of three signals: $P(t)$, the train of pulses eminating from the focus and travelling to a distant recorder; $G(t)$, a similar train of waves reflected from the earth's surface with a reflection coefficient R_H arriving a time Δt behind $P(t)$; and $n(t)$, any other signals present, which are considered to be noise.

$$S(t) = P(t) + G(t) + n(t)$$
$$= P(t) + R_H G(t-\Delta t) + n(t)$$

It is assumed that one of the effects of $G(t)$ is to complicate the seismogram by changing the number and size of peaks and troughs which rise about the background noise level. As a means of identifying $G(t)$ in the seismogram, $S(t)$ is operated on by a series of inverse filters which find an approximation of $P(t)$ for assumed values of R_H, Δt and noise level (u). A concentration ratio, C_R, is calculated for each $P(t)$ found by deconvolution with the inverse filter using the formula

$$C_R = \frac{(\Sigma(\,|P(t)|-u)^2)\text{ for all }|P(t)|>u}{T\,\Sigma(P(t))^2} \qquad (2)$$

where T is the time during which $P(t)$ exceeds u. It is postulated that C_R for a range of Δt's close to the true time delay of the surface reflection, pP, behind the direct compressional pulse, P, from any seismic event will produce a C_R which is greater than the concentration ratio of the original seismogram, C_{RO}.

Preliminary tests showed that for earthquakes and blasts and in scale models a $C_R > C_{RO}$ was usually found at values of Δt and R_H close to what would be expected. It looked, therefore, as though the method might provide a simple means of measuring depth of focus, and, therefore, a simple means of separating blasts from all except the shallowest of earthquakes.

Further tests showed that the situation was not so simple as this. First, it was found that there are five different causes which can produce a value of C_R greater than C_{RO}:

1. Deconvolution removes pP sequence from the seismogram (the solution sought).
2. Deconvolution removes sP sequence or some other sequence than pP.

3. Deconvolution enlarges peaks on the seismogram producing a larger maximum amplitude in the deconvolved seismogram than in the original. (C_R is very sensitive to the height of the largest peak.)

4. Deconvolution cancels out a later half cycle or more of a long oscillatory original seismic pulse.

5. Deconvolution phases random noise so as to add to or subtract from the principal peaks of the seismic pulses.

As a result of this, for any seismogram there are many cases of large C_R, and the right value must be selected from the set. This works out to be a process of testing the deconvolved seismogram, $P(t)$, to determine the cause of each large value of C_R. The third cause in the above list appears to be the major source of false indications. Rules for simple identification are being sought.

The second problem encountered was that in some cases, no large value of C_R was found where the true solution was expected. There are several possible causes for this. First, if R_H is small, the ghost pulse will be lost in the noise. Figure 1 shows the expectable value of R_H as a function of distance from the epicenter for an assumed focal depth of 10 km and the indicated velocity structure. Experience with the method suggests that if $|R_H| < 0.3$, it is unlikely that the ghost can be regularly found in normal seismograms. This means that only seismograms recorded at distances of 22° and beyond will be dependable. This limits the method to events large enough to be recorded beyond 22°.

At the other end of the distance range, the principal seismic pulse recorded beyond 103° has been transmitted thru the earth's core. Wave paths thru the core are complicated, and for most core distances

more than one pulse is recorded. With more than one
P pulse present there is danger of finding Δt's due
to these extra pulses. For this reason, little work
has been done and none is planned on pulses penetrat-
ing into the core.

Another problem is that unless the length of the
filter used in deconvolving the seismogram is several
times as long as the seismogram itself, the decon-
volution is inaccurate and the concentration ratios
found may fail to indentify meaningful solutions.
This was not realized until recently. As a result
many of the tests made for $\Delta t \leq 4$ seconds are undepend-
able and will have to be redone.

A revealing series of tests of the accuracy of the
method was made by testing pulses consisting of one
or more cycles of a sine wave with and without a period
of quiet following the sine waves (Table I). It was
from these tests that it was first learned that decon-
volution could give large values of C_R where there was
peak-enhancement, and that when Δt was small, one had
to be careful that the deconvolution filter, which is
proportional in length to Δt in the computer program
used, was long enough.

Table II summarizes the tests made to date on
nuclear blasts. The tests made for recordings at less
than 3,000 km were early tests, often unsystematic, and
the results are of uncertain value. We have tested all
values of Δt in the ranges given in the table in 0.1
sec intervals unless otherwise stated in the table. It
is necessary to test at intervals which are short
compared to the predominant frequency in the seismograms
or cases where C_R is large may be missed. The digiti-
ing interval used for the seismograms was 0.1 sec in all
cases, though data at half this spacing is available.

The quantity, R, referred to in Table I, is the noise-to-signal power ratio assumed for the seismogram. This is a factor on which the inverse filter which does the deconvolution depends. The pulse length tested is shortened for short Δt's to keep the inverse filter reasonably short. This was not done in the earliest experiments. As a result, there is overlap of the Δt ranges tested as summarized in Table II. It is believed that most of all of the cases of increased C_{RO} reported in Table II will be explainable by one of the reasons listed above. Which case corresponds to which cause is the subject of current study.

Fourier-integral frequency spectra for 24 of the seismograms of Table II have been calculated. The peak frequency and the range for which amplitude is within six decibels of the peak are given in Table III. It is reasonable to expect that testing and sampling intervals should be shorter than one-tenth the period of the peak frequency. No thorough test of how close the sampling interval should be has been made.

To evaluate the Watson-Merdler method it is necessary to compare its depth predictions for blasts with its predictions for earthquakes. To test a given earthquake record thoroughly for all possible amplitude ratios ($R_H = pP/P$) and delay times (Δt) within reasonable limits involves a considerable expenditure of time and money. Initial detailed analysis of the Ecuador earthquake of May 10, 1963, has been restricted to a reasonably small number of amplitude ratios and time delays by considering the following theoretical model. If one assumes that the earthquake can be represented by a point source with energy radiation equal in all

directions, then the theoretical amplitude ratio can be calculated. This assumption is not generally good as energy radiation is known to be dependent on azimuth. A knowledge of the initial radiation pattern (obtainable from fault-plane studies) would serve to improve the model but is not available during this stage of the work. Knowledge of the approximate depth of the disturbance can be used to restrict the range of delay times to be tested. Finally, a measure of the noise level of the seismogram allows one to pick the set of inverse filters designed for that particular noise-to-signal power ratio and to limit the number of noise-energy levels examined in the actual test.

To provide the necessary information for limiting the length of analysis, programs were written to give the following:

(1) The angle of incidence of p at the free surface as a function of epicentral distance for 10 km focal depth (Figure 2). The velocity distribution assumed for this calculation is shown on the Figure.

(2) The amplitude ratio, R_H, of pP/P as a function of the angle of incidence of p at the free surface for various values of Poisson's ratio. The curve for a Poisson's ratio of 0.25 is shown in Figure 3.

(3) Finally, the amplitude ratio of pP/P as a function of epicentral distance was determined and is shown in Figure 1 for a focal depth of ten kilometers.

The pP wave is reversed in polarity compared with P for epicentral distances greater than about 19°, so negative filters are called for. It must be

recognized, however, that the focal mechanism may be such that both pP and P have the same polarity.

Preliminary tests have been carried out on twelve records for the 10 May 1963 Ecuador earthquake using the results from the theoretical calculations based on a point-source model, and some tests have been made on eight additional seismograms. Pertinent results are presented in Tables IV and V. The first five records listed in Table IV were tested for delay times between 2.5 and 12.4 sec corresponding to a depth of focus in the range of about 6 to 49 km. As no significant answers were developed for times greater than 6 sec, initial tests on the remaining seven records were only carried out to 8 sec (about 30 km). Depths less than 6 km have not been tested, as the present set of inverse filters are not designed properly for the small delay times. Table IV shows the theoretical amplitude ratio and measured noise-to-signal power ratio for each record and the filters used in the tests. In all except two cases there was more than one case where C_R exceeded C_{RO}. Only the solutions for the largest C_R's are listed in Table IV. All solutions are shown in Figure 4.

No consistent depth persists throughout Table IV. Values range from 8 to 20 km. The average value is 12 km (compared to 30 km reported by the Coast and Geodetic Survey). In Figure 4, on the other hand, there is a solution between 8 and 12 km in every case except where no solution was found at any depth.

Additional test results using filters with a high noise-to-signal power ratio of 0.25 are included in Table V. The amplitude ratios giving significant answers are in general higher than those listed in

Table IV. The spread in answers is smaller and
there appears to be a preferred depth of about
12 km. Causes of the numerous answers for each
record are being sought as well as a means for
picking the "best" answer.

In addition to those of the 10 May 1963
earthquake, nineteen other seismograms have been
processed thru the Watson-Merdler program. These
are listed in Table VI. The thoroughness of
these tests varies from scattered trial solutions
to systematic tests following the same systems
used for the nuclear blasts. These tests have
been run for a variety of purposes such as for
comparison with nuclear blasts and as checks to
see if any peculiar solutions would result from
various features of the records. They have led
to no conclusions not covered by the previous
discussions of nuclear blasts and the 10 May 1963
Ecuador earthquake.

B. Factors controlling the frequency spectra of
    seismograms

In order to get a better understanding of the
factors which control the frequency spectrum of a
seismogram, a study has been made of the earthquakes
of 13 April 1963 in Peru and 10 May 1963 in Ecuador.
As many seismograms as possible of the beginning of
this earthquake were obtained from the U. S. Coast
and Geodetic Survey and the Dominion Observatory in
Ottawa, Canada. As most of the effort was directed
at the Peru earthquake it will be the only one of
the two for which detailed results will be summarized
here.

Of the paper seismograms obtained for the Peru
earthquake, only ten (five from USCGS and five from

Dominion Observatory) were sufficiently, clearly
and continuously recorded that they could be used
(see Howell, 1965 for discussion of problems of
digitizing paper seismogram). In each case the
seismogram was digitized at tenth-second intervals
for the first 10.0 ± 0.4 sec of the seismogram. Twenty-
seven additional digitized seismograms were obtained
from the United Electrodynamics data center in
Alexandria, Virginia. Fourier-integral frequency
spectra were calculated and a correction for station
sensitivity applied over the frequency range 0.4 to
2.5 cps for each of these 37 seismograms. The range
of epicentral distances was from 4411 km to 11,326
km. Five other Vela stations located in the shadow
zone or further away also gave excellent recordings
but were not included in this study of the P-pulse.

Samples of the corrected frequency spectra are
shown in Figure 5. Except for a general decrease in
energy with increase in frequency, the spectra exhibit
no systematic pattern. Maxima and minima occur in all
cases, but their positions and heights are different
in nearly every case.

A report by W. J. Hannon (1964A and B) led to a
possible explanation of this extreme variability.
Hannon developed a program for computing the effect
of a layered crust on the interference pattern of
continuous plane waves being passed thru it and
reflected at the surface. The spectrum observed at
the surface is the result of interference by the whole
family of internally reflected multiples resulting from
the layering. The effect of these layers on the
spectrum is called the transfer function of the crust.
The transfer function itself is a sequence of maxima

and minima (Figure 6).

Hannon's theory is developed for continuous
waves. A real earthquake is a transient pulse. If
only the first ten seconds of a seismic arrival is
considered, many of the internal reflections contrib-
uting to Hannon's theoretical transfer function will
generally not have had time to arrive. It was, there-
fore, necessary to develop a program for calculating
the transfer function for the case of a finite length
of pulse.

Truncation in the time domain corresponds to
multiplication of the signal by a square window of
unit amplitude during the time duration of the
considered signal, and equal to zero outside this
interval. The transform of such a square window is
a sinc function whose zero-axis crossing will be at
$\frac{1}{T}$ cps, T being the duration in seconds.

Convolution in the frequency domain is equivalent
to multiplication in the time domain. Let $G(f)$ be
the transform for infinite time with $\Theta(f)$ its related
phase spectrum. The truncated spectrum

$$G(f) = G(f)*\mathrm{sinc}(f)$$
$$\left|G_T(f)\right| = ((\mathrm{Re}G(f)*\mathrm{sinc}(f))^2 +$$
$$(\mathrm{Im}G(f)*\mathrm{sinc}(f))^2)^{1/2} \qquad (4)$$

Proper caution must be taken during the convolution
process to reduce as much as possible the error intro-
duced by the truncation of the sinc function. This is
done by extending the real and imaginery parts along
the negative frequency axis before performing the
convolution.

Computer programs were written to generate transfer
functions corresponding to ten seconds in the time
domain for angles of incidence at every 1° within the
range of 20° to 40°. This range includes all expected
angles of incidence for epicentral distances involved

in the study of the 37 spectra.

More than 20 crustal-structure models related
to seven stations were studied. It was found that
certain crustal models have a smooth transfer
function for the whole range of angles of incidence,
while other models, over the same range of angles,
present great differences in the number, the position
and the depth of the minima. Since the crustal effect
acts as a filter on the incoming initial longitudinal
wave, it modifies the frequency spectrum of the pulse
greatly.

The variation of the truncated transfer function
as a function of angle of incidence and of layer
thicknesses was carefully studied by testing nine
closely related models selected on the basis of pub-
lished crustal-structure predictions. It was found
that the transfer function is very sensitive to change
of angle of incidence and layer thickness. The
transfer functions can sometimes introduce minima of
20-30 db, very often of 10 db, thus offering an adequate
explanation for similar minima found in earthquake
spectra.

An attempt was made to find crustal models which
would produce variations similar to those observed
in the spectra at four stations. In two of these
cases, namely Mountain Pine, Ark. and Alert, Canada,
a structure was found whose transfer function, sub-
tracted from the observed spectrum, produced a
demonstrably smoother spectrum than the original.
It is postulated that this model closely resembles
the real crust. Failure to find a model which produced
an improvement for the other two cases is presumably
due to not having hit upon a model which closely

resembles the crust among the many models tested.

Finally, the average spectrum was obtained for
the 37 stations (Figure 9). It shows a remarkable
smoothness in comparison with individual spectra.
This is interpreted as an indication that none of
the minima is introduced by the source function.
Otherwise it would persist and show up on the
average spectrum.

It is concluded that the crustal transfer
function is the dominant cause of variations in
the spectrum from one observing station to another.

C. Scale-model studies of refractions along the
    Mohorovicic discontinuity.

Two scale models were designed and fabricated
as shown in Figure 10. The upper model (A) corres-
ponds to a transition layer underlying a uniform
crust. The lower model (B) corresponds to an
irregular boundary. Model A has been set up in the
model laboratory and is under test.

In Model A an attempt is being made to measure
the transfer characteristics of the two high-speed
interfaces comprising an intermediate velocity layer,
with the distance between these interfaces being of
the same order of magnitude as the predominent wave
length. The frequency band of the study is from 20
kc to 200 kc, which is approximately equivalent to
20 cm to 2 cm wave length in the model. The irregular
boundary at the bottom of the model is an attempt to
reduce reflections occuring at this surface, prevent
the arrival of surface waves that may travel around
the model by this path, and reduce the time that
energy is contained in the model between pulses.

An electronics system capable of providing a
short-duration input to the model was assembled.
The system is able to put out square pulses of as
short a duration as one microsecond and of 150
volts amplitude. Different preamplifiers and even
the cascading of preamplifiers was tried to find
out how much gain would be available when low-energy
refractive arrivals are to be measured. A high
signal-to-noise ratio is necessary, and precautions
had to be taken to ensure low pickup and interfer-
ence. This will become critical at the lowest
energy levels anticipated.

The velocities of compressional waves in the
three layers were measured (Table VII). In addition,
a calculation of the velocity, C_p, in the intermediate
velocity layer (copper-steel lamination) was made
using

$$c_p^2 = \frac{\rho_1 c_{p1}^2 T_1 + \rho_2 c_{p2}^2 T_2}{\rho_1 T_1 + \rho_2 T_2} \tag{5}$$

where ρ_1, C_{p1}, T, are density, compressional wave
velocity, and thickness of material number 1 and where
ρ_2, C_{p2}, T_2 are density, compressional wave velocity,
and thickness of material number 2.

The shear-wave velocities were calculated several
ways, and also roughly measured, with an approximate
value being needed to identify fully the components
present in the preliminary measurements.

Measurements of the absorptive and dispersive
characteristics of the materials were made. This
data is currently under study. Having measurements
for the properties of the steel and the laminated
material, the copper material characteristics can be

inferred. Preliminary evaluation of the data suggests
that the three materials will be low absorptive and non-
dispersive.

D. Attentuation of seismic waves under Lake Superior

Fourier-integral frequency spectra were calculated
for the range 4-26.8 cps for first arrivals in two
distance ranges: 35-82 km and 158-252 km for seismic
pulses refracted under Lake Superior. The first case
is interpreted as a direct pulse, the second as a
refracted (head) wave in an intermediate (7.00 km/sec)
layer. The absorption coefficient in the first case
was found not to be significantly different from zero
($\alpha = (-0.010151 - .00059F)$/km, where F is frequency).
In the second case, absorption was larger but not signif-
icantly dependent on frequency ($\alpha = (0.006620 - 0.00011F)$/km).
The refracted pulse was weaker in energy above 8.8 cps
than the direct pulse. This is similar to the filtering
effect observed in the Maine seismic experiment and is
explainable, using Nakamura's theory, by a transition
layer 0.16 km thick. (Nakamura, 1964; Nakamura and
Howell, 1964). A report summarizing this is in press
(Howell, 1966A).

E. Publications and oral reports

In addition to the reports required by this contract,
during 1965 the following papers were presented orally
or in writing thru the indicated media, thereby dissemi-
nating knowledge gained thru this research.

1. Robert J. Watson presented a paper describing the
Watson-Merdler method of focal-depth analysis before a
VESIAC conference in La Jolla on March 23. The proceed-
ings of this conference have not yet been published, but
are to be issued in 1966.

2. B. F. Howell, Jr. presented a paper before the Seismological Society of America discussing some of the problems of obtaining digitizable seismograms using paper recordings. This paper has been published in Earthquake Notes (Howell, 1965).

3. B. F. Howell, Jr. presented a paper before the Seismological Society of America describing the digitizing apparatus developed in the research and used for digitizing seismograms. This paper (Howell, 1966B) will be published shortly and distributed as a scientific report.

4. B. F. Howell, Jr. has prepared a report of his analysis of the frequency spectra of seismic refractions under Lake Superior. This is being submitted for publication in the Merle A. Tuve Testimonial Volume of the Carnegie Institution of Washington.

III. PERSONNEL

The personnel engaged in this research during the past year consisted of Professors B. F. Howell, Jr., P. M. Lavin, and R. J. Watson and six graduate assistants: Y. Y. Cheng, G. Leblanc, J. L. Lin, T. W. Novotny, D. E. Siskind, and S. K. Yiu. Professor Howell has been guiding the studies of actual earthquakes by Leblanc, and Yiu and the scale-model work of Siskind. Professor Lavin has guided the scale model experiments of Novotny and an evaluation of the Watson-Merdler method as applied to the 10 May 1963 earthquake by Cheng. Professor Watson directed Mr. Lin in evaluating the Watson-Merdler method of depth-of-focus calculation for nuclear blasts until he resigned in July; Professor Howell has directed Lin since then. Professor Howell has been studying the spectra of pulses refracted thru the earth's crust under Lake Superior.

IV. Problems Encountered

We have been plagued throughout the work by slow delivery of parts and equipment. During part of the past month the University's computer has been closed. As a result, we are behind schedule and have had to obtain an extension of time to complete the proposed work.

V. Schedule of work and future plans

The research planned for the remainder of this project consists primarily of three experiments: 1. study of the cause of large values of C_R for deconvolved blast seismograms; 2. study of the 10 May 1963 earthquake; and 3. model studies of refraction along the Mohorovicic discontinuity.

Fourteen nuclear-blast seismograms recorded at large distances from the epicenter are on hand. All are being systematically tested using a standard procedure. In all cases where C_R exceeds C_{RO}, the deconvolved seismogram will be compared with the original seismogram to see exactly why the Watson-Merdler method picked this case as a potential solution. If all potential solutions have obvious explanations, the Watson-Merdler method can be used as a criterion to select blast records from a group of seismograms of unknown source nature.

The work on earthquake seismograms will follow similar lines. An explanation will be sought for all large values of C_R for the 10 May 1963 Ecuador earthquake and for a few other individual shocks. For the Watson-Merdler method to be successful, it will ϶ necessary that natural earthquakes commonly produce large C_R values which cannot be easily

explained as being other than the result of
combinations of pulses.

Data from the scale models simulating refractions
along the Mohorovicic discontinuity will be taken
during the coming quarter. Analysis of this data
should be complete by June.

Several reports are under preparation. A
Complete technical report and one or more scientific
reports on the cause of variations in the frequency
spectra of the 13 April 1963 Peru earthquake, including
the program for deriving the truncated transfer function
for a layered crust, is being written. Also, a
scientific report on the spectra of refractions under
Lake Superior is nearing completion. Some additional
research on this latter problem continues, especially
as it relates to absorption of seismic waves. This
may lead to an additional report later.

VI. Actions desired of ARPA

A proposal to extend this research thru December,
1966, either with or without additional funds, was
submitted a year ago and has never been acted on
formally. It now looks as though funds already approved
will be adequate to complete what needs to be done on
this research. Although actual research should be
completed by June of 1966, it is still desired the
contract-terminated date should be postponed until
31 December 1966. This will permit the final reports
to be prepared more carefully and thoroughly than will
be possible if they must be in by June. Also, it will
permit preparation and submission of a series of
scientific reports for publication in journals where
the information they contain will reach the largest
number of scientists and will become a matter of con-
venient permanent record.

References

Hannon, W. J., 1964A, An application of the Haskell-Thomson matrix method to the synthesis of the surface motions due to dilatational waves. Bull. Seis. Soc. Am. 54:2067-2079.

Hannon, W. J., 1964B, Some effects of a layered system on dilatational waves. AFCRL Report 64-614.

Howell, B. F., Jr., 1965, Optimum sensitivity for seismographs. Earthquake Notes 16:7-8.

Howell, B. F., Jr., 1966A, Lake Superior Seismic Experiment: Frequency Spectra and Absorption. The Tuve Testimonial Volume, Carnegie Institution of Washington (in press).

Howell, B. F., Jr., 1966B, Simple digitizer for paper seismograms. In press, April issue of Bulletin of the Seismological Society of America.

Nakamura, Y., 1964, Model experiments on refraction arrivals from a linear transition layer. Bull. S.   Soc. Am. 54:1-8.

Nakamura. Y.; B. F. Howell, Jr., 1964, Maine seismic experiment; frequency spectra of refraction arrivals and the nature of the Mohorovicic discontinuity. Bull. Seis. Soc. Am. 54:9-18.

Table I

Cases where Watson-Merdler program found $C_R > C_{RO}$ for a sine wave of

two seconds period

Cycles	Length of pulse (sec)	Delays for which energy concentrations are larger than zero delay (sec)	Input delay (sec)
1	2	0.6, 1.0	0.2-3.2 in steps of 0.2
2	4	0.2, 1.0, 1.4	" " " " "
3	6	0.2, 1.0, 3.0	" " " " " "
4	8	1.0, 2.6, 1.6	" " " " "
5	10	1.0, 2.5, 3.3, 5.0	0.8-6.0 in irregular steps
6	12	0.2, 2.4, 3.0	0.6-6.0 in irregular steps
8	16	0.2, 2.6, 3.6, 4.6, 5.4	0.2-6.0 in irregular steps
10	20	0.2, 4.4, 5.0	" " " "
12	24	0.2, 3.0, 4.4	" " " "

TABLE II

Summary of Tests Made on Nuclear Blasts

Event number	Station	Distance	Pulse Length sec.	Input Delay Time (Δt) sec.	Input R_H + Input R	Delay for which C_R's are larger than C_{RO}'s	RH
Bilby (29)	LZBV	8,000 km	40	0.1-8.0	R_H= -0.4,-0.5,-0.7, -0.9 R = 0.25	0.9,1.6,2.3,5.9,7.4	-0.9
Bilby (29)	LZBV	8,000 km	28	8.0-14.5	R_H= -0.4,-0.6,-0.8, R = 0.01	No solution	
Bilby (30)	OONW	8,122 km	40	0.1-5.0	R_H= -0.4,-0.6,-0.8, -1.0 R = 0.25	0.7,1.1,2.2,3.5	-1.0
Bilby (30)	OONW	8,122 km	28	4.1-14	R_H= -0.5,-0.7,-0.9, R = 0.0625	9.1	-0.5
Bilby (30)	OONW	8,122 km	19.6	2.0-4.0	R_H= -0.5,-0.7,-0.9 R = 0.0625	2.1,2.2	-0.5
Bilby (30)	OONW	8,122 km	9.8	1.0-2.0	R_H= -0.5,-0.7,-0.9 R = 0.0625	1.0,1.3,1.4	-0.9
Bilby (31)	SBGR	8,000 km	40	0.1-10	R_H= -0.4,-0.6,-0.8, -1.0 R = 0.25	0.6,1.0,2.1,2.4,3.3, 8.3	-1.0
Bilby (31)	SBGR	8,000 km	28	8.0,14	R_H= -0.4,-0.6,-0.8 R = 0.0625	12.6	-0.4
Bilby (31)	SBGR	8,000 km	19.6	2.0-4.0	R_H= -0.5,-0.7,-0.9 R = 0.01	3,3,3,4	-0.5

Table II - continued

Event number	Station	Distance	Pulse Length sec.	Input Delay Time (Δt) sec.	Input R_H + Input R	Delay for which C_R's are larger than C_{RO}'s	RH
Bilby (32)	HWIS	5,199 km	40	0.1-10	R_H= -0.5,-0.7,-0.9 R = 0.25	0.6,1.2,1.6,4.7	-0.9
Bilby (32)	HWIS	5,199 km	28	8.0-14	R_H= -0.4,-0.6,-0.8 R = 0.25	No solution	·
Bilby (32)	HWIS	5,199 km	19.6	2.0-4.0	R_H= -0.5,-0.7,-0.9 R = 0.25	No solution	
Bilby (33)	CPO	2,725 km	40	0.1-8.0	R_H= -0.4,-0.6 R = 0.25	0.5,0.9,1.6,4.3,5.9	-0.4
Bilby (33)	CPO	2,725 km	28	8.0-14	R_H= -0.4,-0.6,-0.8 R = 0.01	12.6	-0.4
Bilby (33)	CPO	2,725 km	19.6	2.0-4.0	R_H= -0.5,-0.7,-0.9 R = 0.0625	2.0,2.2	-0.5
Bilby (307)	EKA-2	7,967 km	28	4.1-14	R_H= -0.5,-0.7,-0.9 R = 0.0625	4.1,4.2	-0.5
Bilby (307)	EKA-2	7,967 km	19.6	2.0-4.0	R_H= -0.5,-0.7,-0.9 R = 0.0625	2.2,2.3,2.4,2.5,3.1, 3.7	-0.5
Bilby (307)	EKA-2	7,967 km	9.8	1.0-2.0	R_H= -0.5,-0.7,-0.9 R = 0.0625	1.5,1.6	-0.5
Shoal (34)	BMO	634 km	40	0.1-8.0	R_H= -0.5,-0.7,-0.9 R = 0.25	0.6,1.6,2.2,3.2	-0.7

Table II - continued

Event number	Station	Distance	Pulse Length sec.	Input Delay Time (Δt) sec.	Input R_H + Input R	Delay for which C_R's are larger than C_{RQ}'s	RH
Shoal (35)	CPO	2,915 km	40	0.1-10.0	R_H = -0.5, -0.7 R = 0.25	1.0,1.1,3.9	-0.7
Shoal (36)	WMO	1,826 km	40	0.1-10.0	R_H = -0.5,-0.6,-0.8 R = 0.25	0.9,1.8,2.6,3.1	-0.6
Shoal (37)	LZBV	8,012 km	30	0.1-10	R_H = -0.5,-0.7,-0.9 R = 0.25	0.9,5.2,5.6,7.6,8.6	-0.1
Shoal (262)	DHNY	4,000 km	30	0.1-10	R_H = -0.5,-0.7,R=0.25	0.7,0.9,1.3,6.5	-0.7
Shoal (268)	RYND	1,700 km	30	0.1-8.0	R_H = -0.4,-0.6,-0.8 R = 0.25	0.7,1.4,2.3,3.1,4.7,6.4	-0.8
Shoal (261)	RKON	2,300 km	30	0.7-9.8	R_H = -0.4,-0.5,-0.7,-0.9 R = 0.25	0.8,2.0,2.8	-0.5
Shoal (325)	NPNT		28	4.1-14	R_H = -0.5,-0.7-0.9. R = 0.0625	7.2,11.9	-0.5
Shoal (325)	NPNT		19.6	2.0-4.0	R_H = -0.5,-0.7,-0.9 R = 0.0625	No solution	
Shoal (325)	NPNT		9.8	1.0-2.0	R_H = -0.5,-0.7,-0.9 R = 0.0625	1.2	-0.5
Aardvark (257)	LCNM	1,000 km	30	0.8-9.6	R_H = -0.4,-0.5,-0.7, -0.9 R = 0.25	1.6,2.4,4.0,7.2	-0.7
Aardvark (266)	WNSD	1,500 km	30	0.7-7.7	R_H = -0.4,-0.5,-0.7, -0.9 R = 0.25	2.1,4.2	-0.4

Table II - continued

Event number	Station	Distance	Pulse Length sec.	Input Delay Time (Δt) sec.	Input R_H + Input R	Delay for which C_R's are larger than C_{RO}'s	RH
Aardvark (258)	MNW	500 km	30	0.8-9.6	R_H= -0.4,-0.5,-0.7, -0.9 R = 0.25	1.6,4.0	-0.4
Aardvark (270)	RKMS	2,500 km	30	0.5-13.0	R_H= -0.4,-0.5,-0.7, -0.9 R = 0.25	0.5,1.5,3.0	-0.9
Hardhat (259)	BLWV	3,000 km	30	0.1-10	R_H= -0.5,-0.7,-0.9 R = 0.25	1.2,1.7,2.4,4.9,5.8, 8.6	-0.9
Hardhat (264)	RTUN	1,300 km	30	0.7-7.7	R_H= -0.4,-0.5,-0.7 -0.9 R = 0.25	1.4	-0.4
Haymaker (267)	WMO	1,600 km	30	0.7-8 4	R_H= -0.4,-0.5,-0.7, -0.9 R = 0.25	1.4,2.8,4.9	-0.7
Salmon (260)	BMO	1,700 km	30	0.1-10	R_H= -0.4,-0.5,-0.7 R = 0.25	0.7,1.8,2.4,5.3,7.0, 7.6,9.0	-0.5
Salmon (269)	DRCO	1,700 km	30	0.6,1.3,1.8,2.4,3.0,3.6, 4.2,4.8,5.4,6.0,6.6,7.2, 7.8,8.4,9.0	R_H= -0.4,-0.5,-0.7, -0.9 R = 0.25	0.6,3.0	-0.9
Salmon (263)	RMON	2,250 km	30	0.1-10	R_H= -0.4,-0.5,-0.7 R = 0.25	1.7,2.3,3.7,4.5,5.5	-0.7
Salmon (265)	UBO	2,100 km	30	0.8,1.6,2.4,3.2,4.0,4.8, 5.6,6.4,7.3,8.0,8.8,9.6, 10.4,11.0	R_H= -0.4,-0.5,-0.7, -0.9 R = 0.25	2.4	-0.7

Table II - continued

Event number	Station	Distance	Pulse Length sec.	Input Delay Time (t) sec.	Input R_H + Input R	Delay for which C_R's are larger than C_{RO}'s	RH
Salmon (256)	BLWV	1,100 km	30	0.8-9.6 increment with 0.8 sec.	$R_H = -0.4, -0.5, -0.7, -0.9$ $R = 0.25$	0.8,2.4	-0.5
Mississippi (313)	HN-ME	4,070 km	28	4.1-14	$R_H = -0.5, -0.7, -0.9$ $R = 0.25$	4.2,4.3,4.4,4.5,4.6, 6.2,6.3,6.4,12.9	-0.9
Mississippi (313)	HN-ME	4,070 km	19.6	2.0-4.0	$R_H = -0.5, -0.7, -0.9$ $R = 0.25$	3.0,3.1,3.2	-0.9
Mississippi (313)	HN-ME	4,070 km	9.8	1.0-20	$R_H = -0.5, -0.7, -0.9$ $R = 0.25$	1.3	-0.9
Salmon (305)	NPNT	5,264 km	28	4.1-14	$R_H = -0.5, -0.7, -0.9$ $R = 0.0625$	7.7,7.8,8.0 8.6,9.0,12.6	-0.9 -0.5
Salmon (305)	NPNT	5,264 km	19.6	2.0-4.0	$R_H = -0.5, -0.7, -0.9$ $R = 0.0625$	2.7,2.8,3.5	-0.5
Salmon (305)	NPNT	5,264 km	9.8	1.0-2.0	$R_H = -0.5, -0.7, -0.9$ $R = 0.0625$	1.2,1.3	-0.5

Table III

Peak of Frequency Spectrum of Seismograms of Blasts

Event and number	Station	Distance	6 DB down maximum at left side	F max	6 DB down maximum at right side
Bilby (29)	LZBV	8000 km	0.525	0.775	1.1
Bilby (30)	OONW	8122 km	0.525	0.625	0.75
Bilby (31)	SBGR	8000 km	0.775	0.825	0.85
Bilby (32)	HWIS	5199 km	0.70	0.725	0.825
Bilby (33)	CPO	2725 km	0.55	0.6	0.675
Shoal (34)	BMO	634 km	1.275	1.45	2.2
Shoal (35)	CPO	2915 km		0.225	0.325
Shoal (36)	WMO	1826 km	0.725	0.875	0.95
Shoal (37)	LZBV	8012 km		0.25	0.325
Shoal (262)	DHNY	4000 km	0.94	1.03	1.17
Shoal (268)	RYND	1700 km	1.12	1.17	1.42
Shoal (261)	RKON	2300 km	1.26	1.32	1.36
Salmon (256)	BLWV	1100 km	2.78	2.8	3.05
Salmon (260)	BMO	1700 km	0.21	0.3	0.56
Salmon (263)	RMON	2250 km	2.32	2.42	2.52
Salmon (265)	UBO	2100 km	0.46	0.56	0.71
Salmon (269)	DRCO	1700 km	0.44	0.6	1.18
Aardvark (257)	LCNM	1000 km	0.83	0.88	0.92
Aardvark (258)	MMTW	500 km	1.05	1.12	1.19
Aardvark (266	W3D	1500 km	0.84	0.87	0.9

Table III - continued

Event and number	Station	Distance	6 DB down maximum at left side	F max	6 DB down maximum at right side
Aardvark (270)	NLWS	2500 km	0.86	0.98	1.07
Hardhat (259)	BLWV	3000 km	2.13	2.19	2.4
Hardhat (264)	RTUN	1300 km	1.35	1.5	1.53
Haymaker (267)	WMO	1600 km	0.67	0.82	1.1

Table IV

Focal depths indicated for the Ecuador Earthquake of 10 May 1963

Series	Sta.	Δ°	Expected Values		Filter Tested			Results			
			pP/P	Noise-signal power ratio (R)	R	pP/P	u	Δt	pP/P	u	h
7	AAM	44.63	-0.54	.072	.0625	-.5	.2, .3	3.5	-.5	.2	10.8
						-.7		5.6	-.5	.3	20.0
12	SCP	42.80	-0.53	.015	.01	-.5	.1, .2	2.8	-.5	.1	8.2
						-.7		3.7	-.5	.2	11.8
101	PHC	67.67	-0.71	.038	.0625	-.5	.2, .3	3.9	-.9	.3	11.5
						-.7		3.0	-.7	.2	8.3
						-.9					
113	RES	77.48	-0.81	.055	.0625	-.5	.1, .2	No significant solution			
						-.7					
102	VIC	64.24	-0.69	.005	.01	-.5	.1, .2	3.1	-.7	.2	8.3
						-.7					
9	CMC	74.59	-0.75	.012	.01	-.7	.1, .2	No significant solution			
						-.9					
5	STU	89.52	-0.82	.054	.0625	-.8	.2, .3	5.1	-.8	.3	15.3
						-1.0		3.8	-.8	.3	10.9
8	PTO	75.79	-0.75	.055	.0625	-.5	.2, .3	4.6	-.7	.2	14.2
						-.7					
13	WID	93.51	-0.83	.095	.125	-.6	.3, .4	2.9	-.8	.3	7.7
						-.8		3.6	-.8	.4	9.9
99	ALE	20.88	-0.81	.012	.0625	-.6	.1, .2	3.4	-.6	.2	9.4
						-.8					

Table IV - continued

Series	Sta.	Δ°	Expected Values		Filter Tested			Results			
			pP/P	Noise-signal power ratio (R)	R	pP/P	u	Δt	pP/P	u	h
100	LDN	45.15	-0.54	.184	.25	-.5	.3, .4	4.2	-.6	.4	14.1
						-.6		2.7	-.5	.4	8.1
103	MBC	81.86	-0.79	.002	.01	-.6	.1, .2	3.0	-.6	.2	3.2
						-.8		3.9	-.6	.2	11.2

TABLE V

Additional depth predictions for the 10 May 1963

Ecuador Earthquake:

No.	Station (code)	Δ (EM)	RH	U-level	Delay time (sec)	Focal depth (km)
7	Ann rbor (AAM)	4,959	-1.0	.3	3	8
			-0.8	.4	5.5	16.5
9	Copper Mine (CMC)	8,288	-0.6	.5	4	12
5	Stuttgart (STU)	9,947	-1.0	.4	6	18
8	Porto (PTO)	8,421	-0.8	.1	4	12.5
13	Windhook (WIN)	10,389	-0.8	.3	3	10
99	Alert (ALE)	--	--	--	--	--
100	London (LDN)	5,016	-1.0	.1	3.5	11
103	Mould Bay (MBC)	9,096	-0.8	.1	3.5	11
101	Port Hardy (PHC)	7,519	-1.0	.4	4	12
113	Resolute Bay (RES)	--	--	--	--	--
102	Victoria (VIC)	7,138	-0.8	.5	4	12
163	Manhatten (MHT)	9,418	-0.6	.2	2.7	7.2
					3.1	8.4
					3.5	9.8
					4.0	11.4

TABLE V - continued

No.	Station (code)	Δ (EM)	RH	U-level	Delay time (sec)	Focal depth (km)
162	Cape Girardeau (CGM)	9,769	-0.6	.2	2.8 3.9 5.6	7.4 11.1 17.1

The following solutions are possibly paired core phases:

No.	Station (code)	Δ (EM)	RH	U-level	Delay time (sec)	Focal depth (km)
14	Charles Tower (CTA)	14,625	-0.6 -0.6	.4 .5	3 5.5	9 14.5
10	Chieng Mai (CHG)	18,181	-0.6	.1	2.5	6.5
15	Baguio (BAG)	17,468	-0.8	.2	7	21
11	Mundaring (MUN)	15,952	-0.6	.4	3.5	1.0
6	New Dehli (NDI)	16,040	-0.6	.1	4.0	12

Table VI

Watson-Merdler Solutions for Earthquakes Other Than Ecuador 10 May 1963

number	Date	Location	at	Comp.	Rough distance (km)	USCGS depth (km)	"Best" solution			Rough Predicted depth (km)
							ΔT	R_H	u	
1	14 JY 62	Kurile Is.	SCP	SPZ	-	60	12.7	-1.0	-	45
2	23 JY 62	Costa Rica	SCP	SPZ	3500	44	6.9 or 8.7	-0.8	-	23 or 32
3	23 AU 62	Alaska	SCP	SPZ	-	10	3.3	-0.8	-	10
4	17 NO 62	Mex.-Guat.	SCP	SPZ	-	12	4.9	-0.8	-	15
38	6 OC 62	Ecuador	WMO	SPZ	(4800)	149	25			(130)
39	6 OC 62	Ecuador	LCNM	SPZ	(4800)	149	25.5			(130)
40	5 OC 62	Ecuador	BMO	SFZ	(4800)	149	25.5			(130)
41	6 FE 64	Sumba	SCP	SPZ	-	43	11.5	-0.6	0.4	45
56	14 OC 63	Kurile Is.	SCP	SPZ	9351	50	No significant solutions			-
71	27 OC 63	Kamchatka	SCP	SPN	8000	--	0.5	-	-	--
141	2 JY 63	Ecuador	ARE	Z	-	33	4	-0.7	.	14
144	2 JY 63	Ecuador	CAR	Z	-	33	10.4	-0.4	-	37
237	9 JY 63	Costa Rica	ARE	Z	-	31	10.4	-0.9	-	40
156	1 SE 62	Rat Is.	SCP	SPZ	11500	-	1.6	-0.9	0.1	4
173	9 JY 63	Panama	SLM	Z	3500	31	1.8	-0.8	0.3	6
176	25 OC 62	Panama	MIT	SPZ	3800	51	14.4	-0.4	0.2	58
177	25 OC 62	Panama	BCU	SPZ	3200	51	12.8	-0.9	0.3	50
300	20 JY 62	Fallon	WMO	LI	1822	33	9.6	-0.5	0.3	50
317	10 JY 63	Georgian SSR	BMO	ZI	10037	17	5.7	-0.7	-	18

Velocities in the Models

TABLE VII

Material	Thickness	Measured Vel. of compr. waves	Calculated Vel. of compr. waves	Calculated Vel. of shear waves
Copper plate	0.64"	3980 M/S	-----	1860-2200
Steel plate	0.32"	5450	-----	3000-3300
Copper-steel lamination	0.64"-0.32"	4510	4520	2500-2700

h = 10 km
σ = 0.25

Velocity Distribution

Depth (km)	Vp (km/sec)
5	5.80
10	5.85
15	6.10
20	6.42
25	6.70
30	7.62
35	8.15
40	8.05
50	7.95

Amp. Ratio of pP/P (R_r)
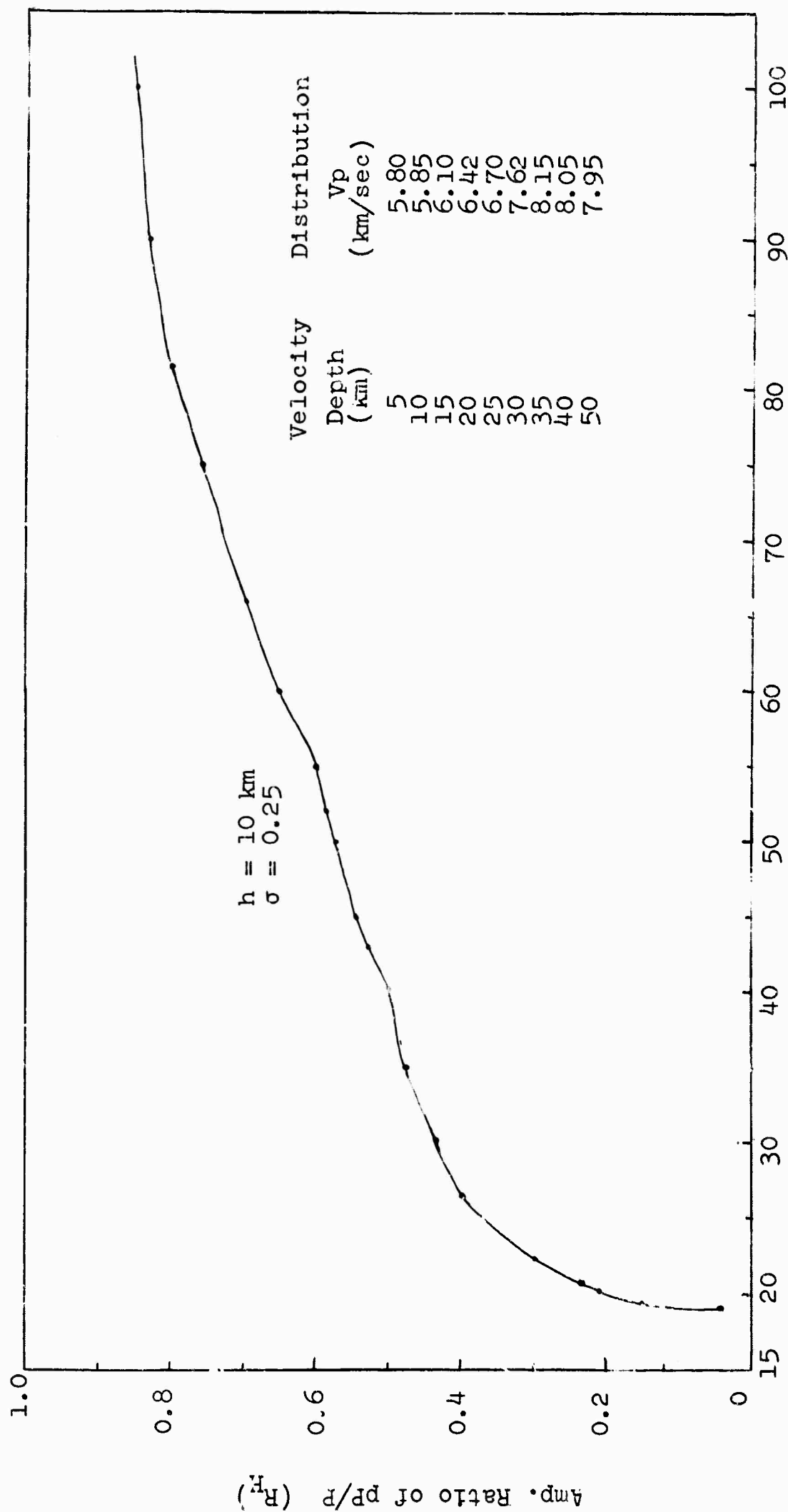
Epicentral Distance (Degrees)
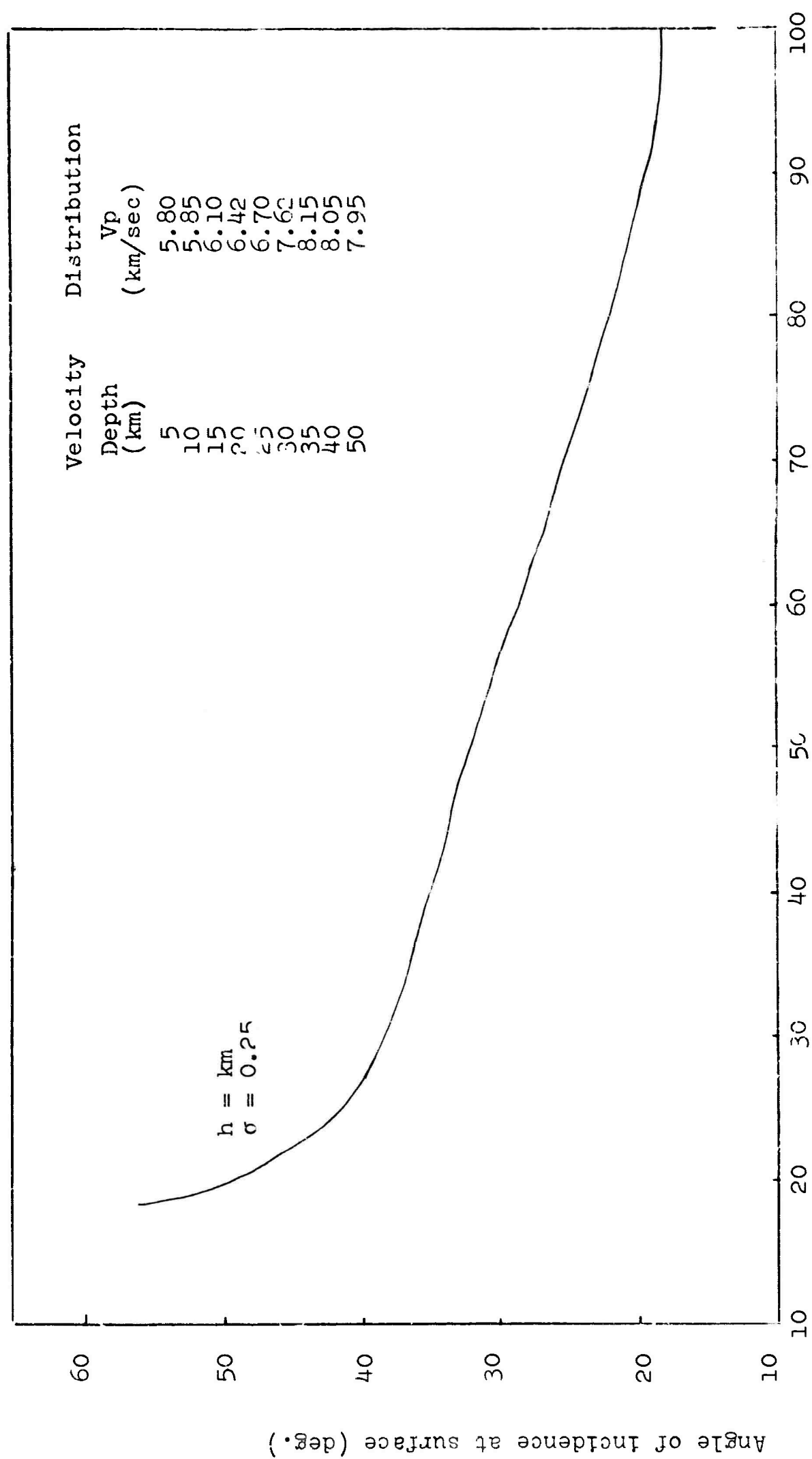
Figure 1

Figure 2. Angle of incidence of P vs. epicentral distance
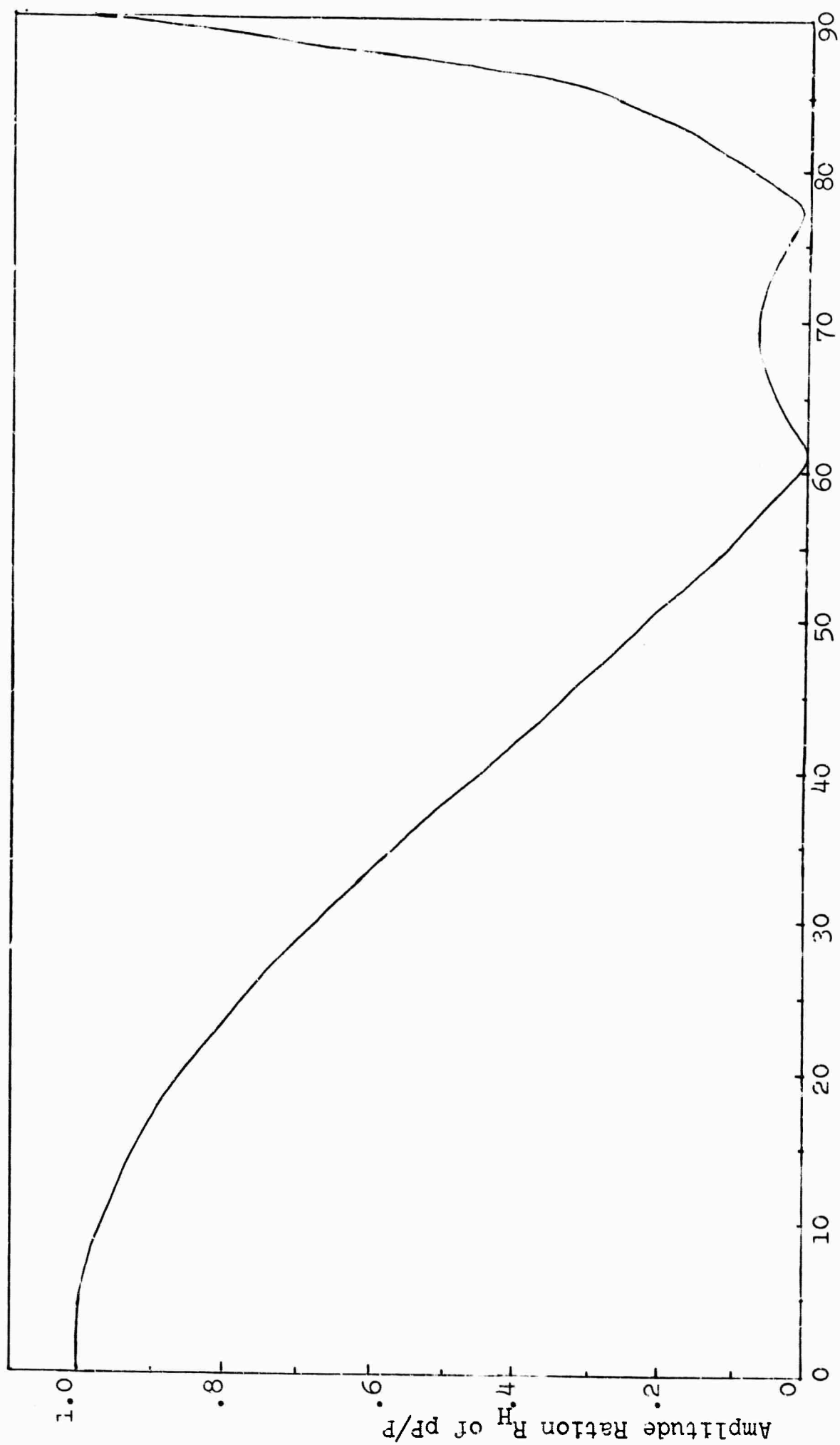
Figure 3. Angle of incidence at reflection point for $\sigma = .25$
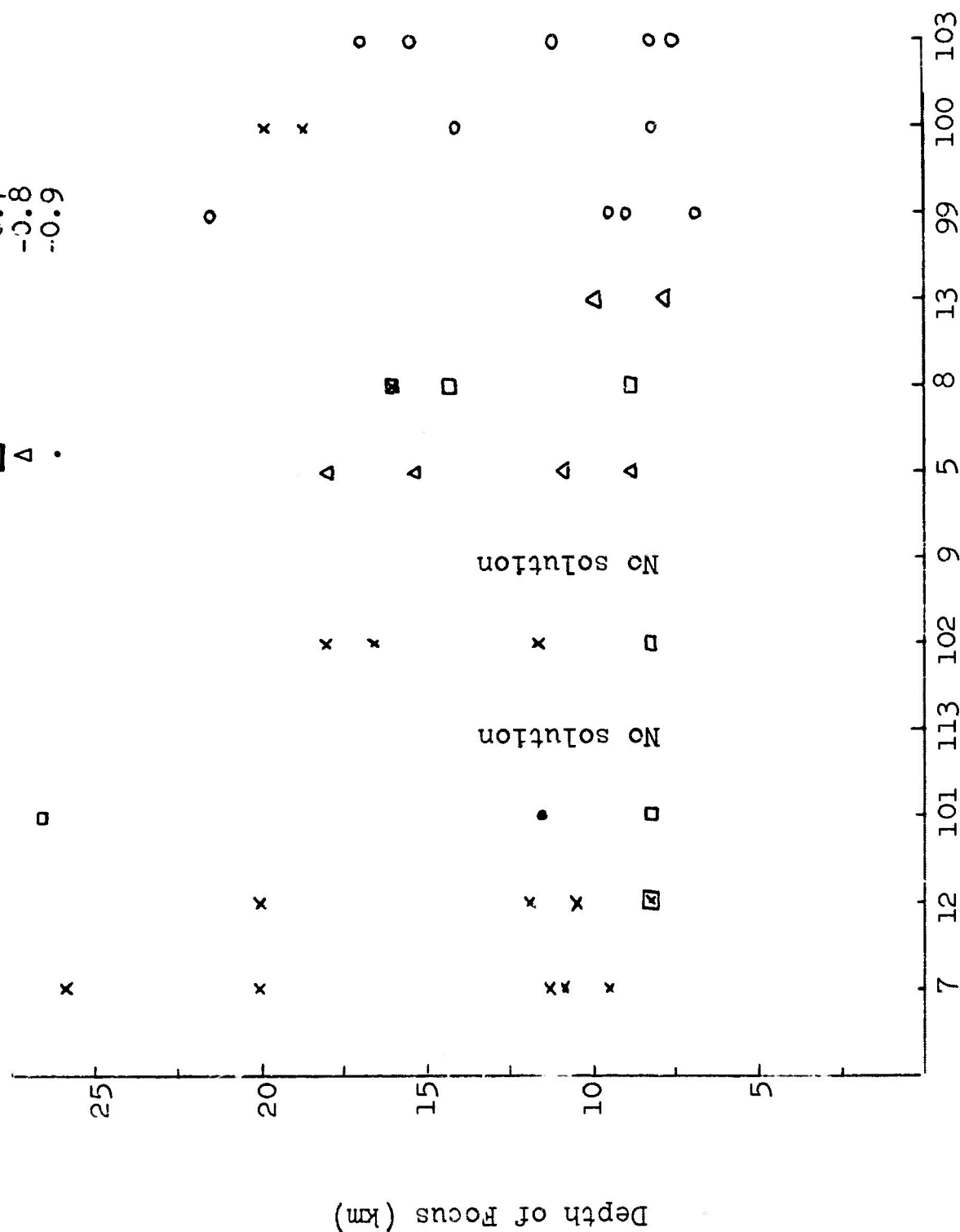
Figure 4. Chart of cases where C_R exceeds C_{RO} for seismograms listed in Table 4.

Figure 5. Spectra of Peru Earthquake at three different stations.

LCNM
WTTN
HNME

Frequency in cps

Relative amplitude in decibels

-36
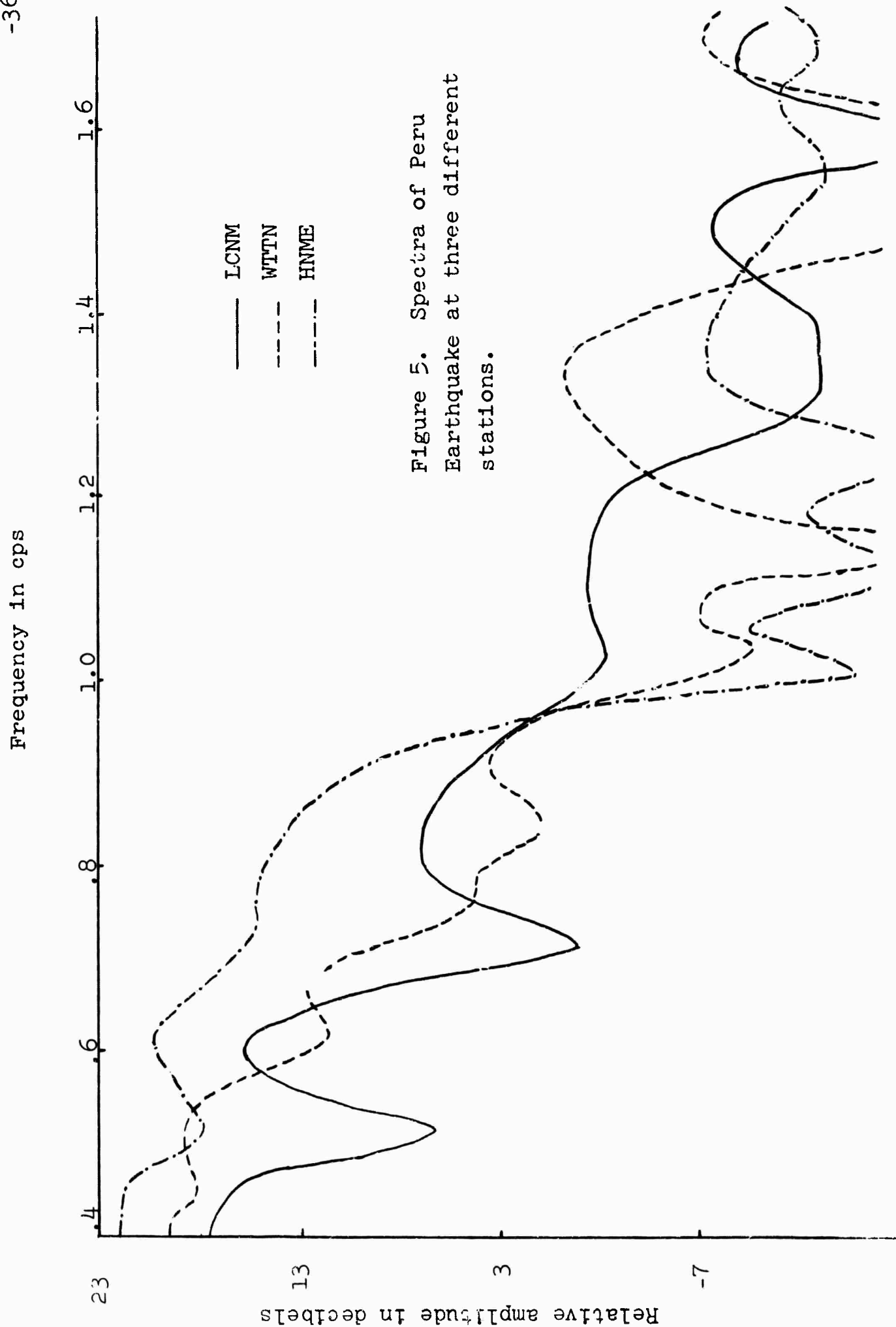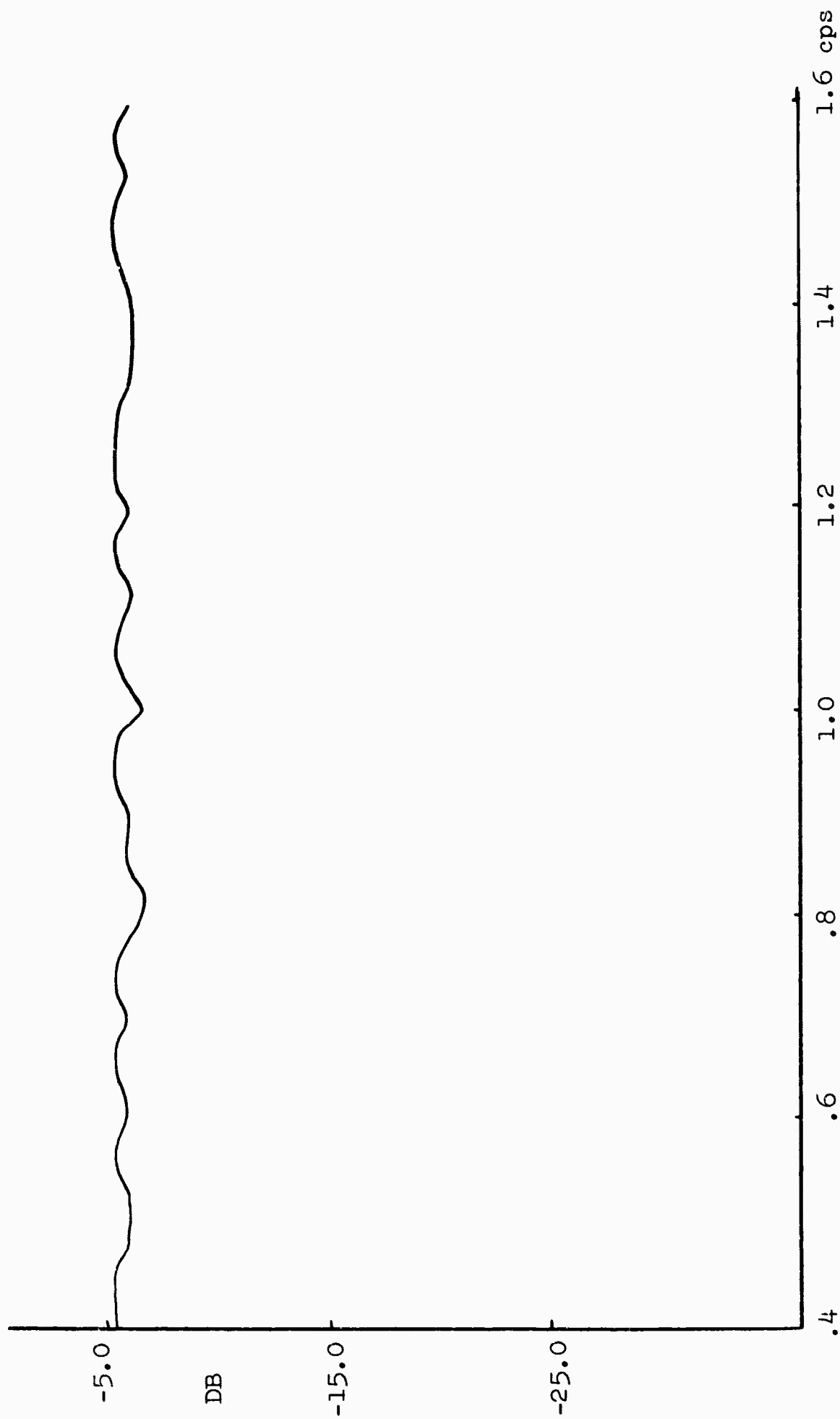
Figure 6. Truncated transfer function for Ontario, Angle 1 = 30°.
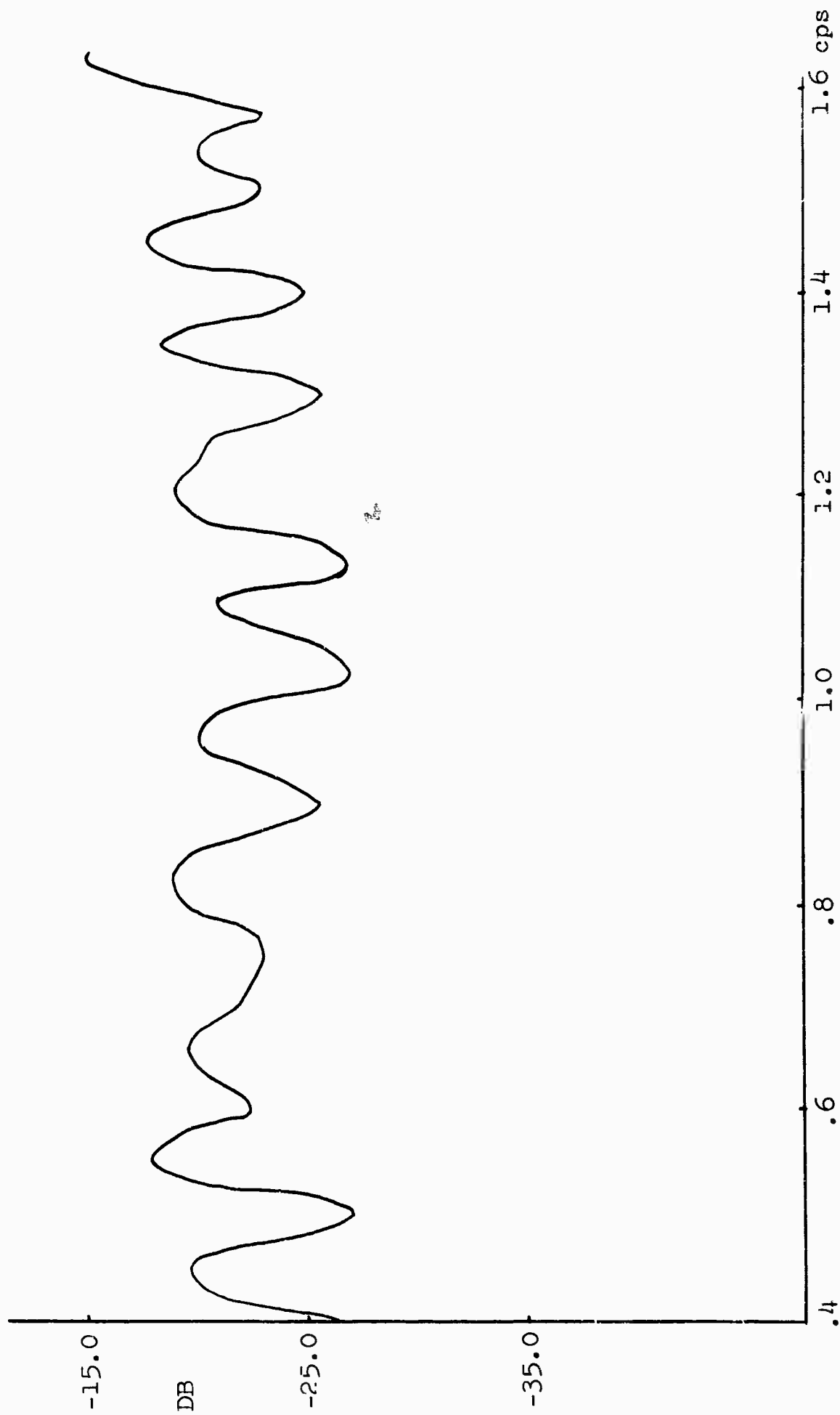
Figure 7. Truncated transfer function for Model 7.4, Angle 1 = 33°.
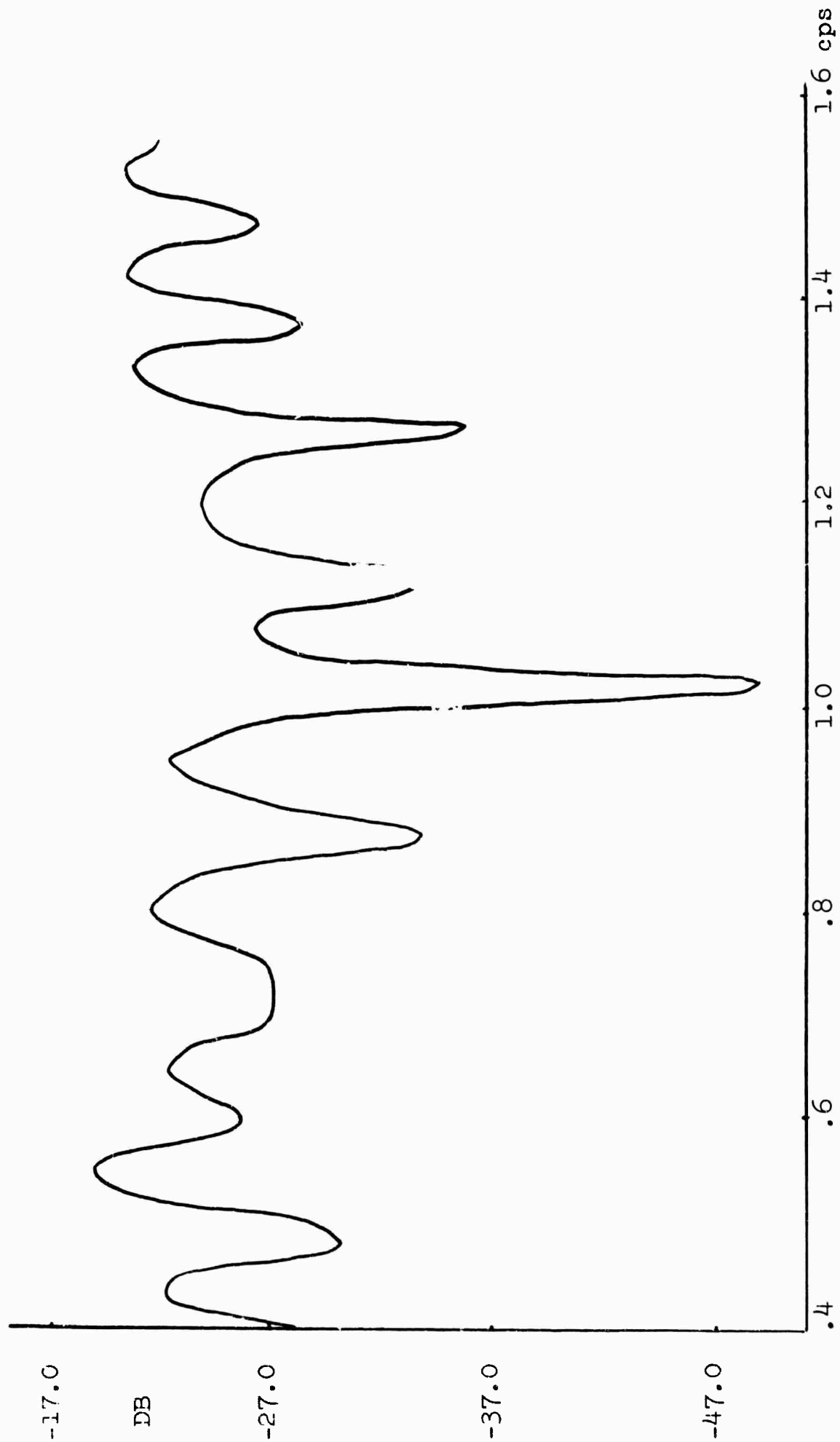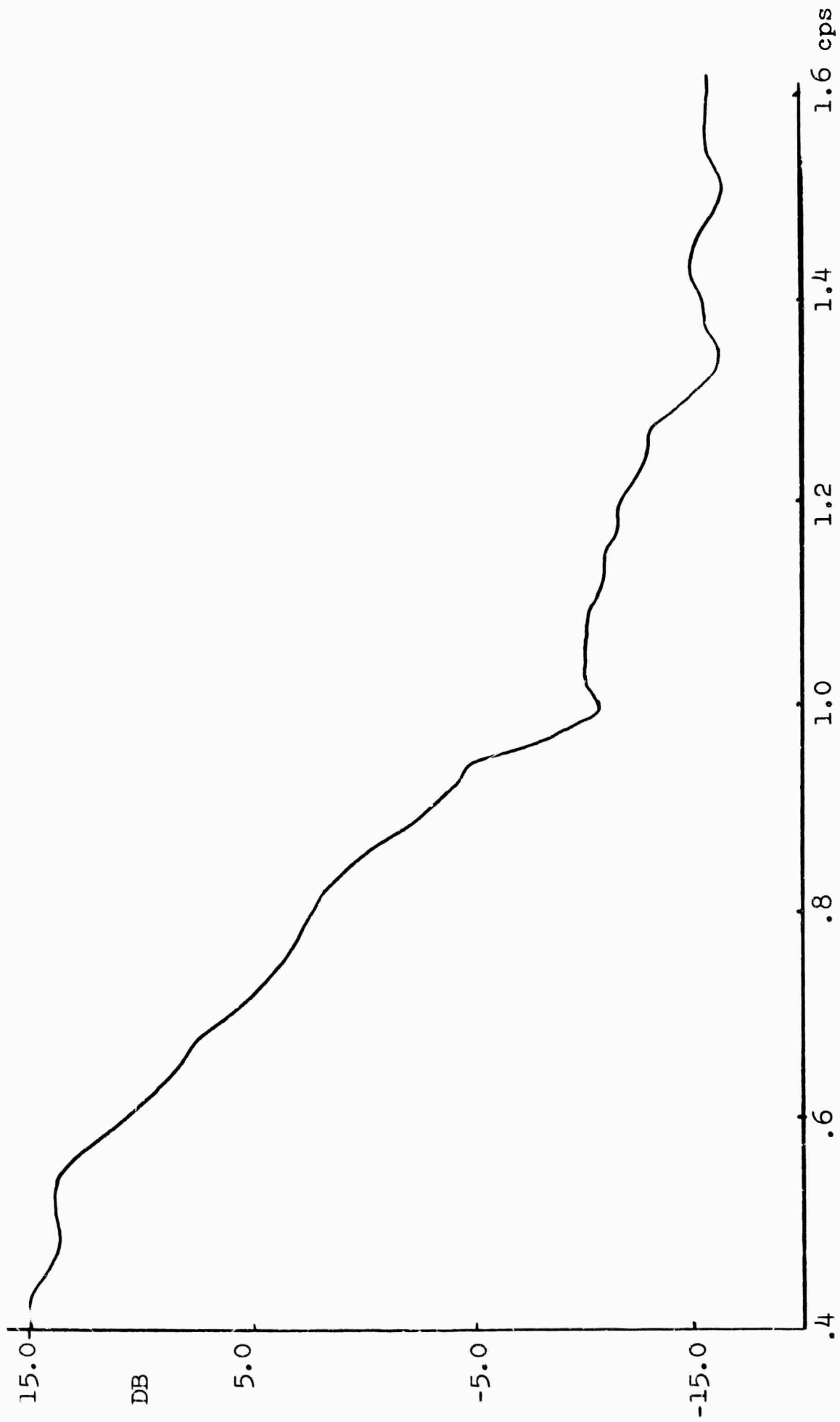
Figure 8. Truncated transfer function for Model 7.4, Angle i = 34°.
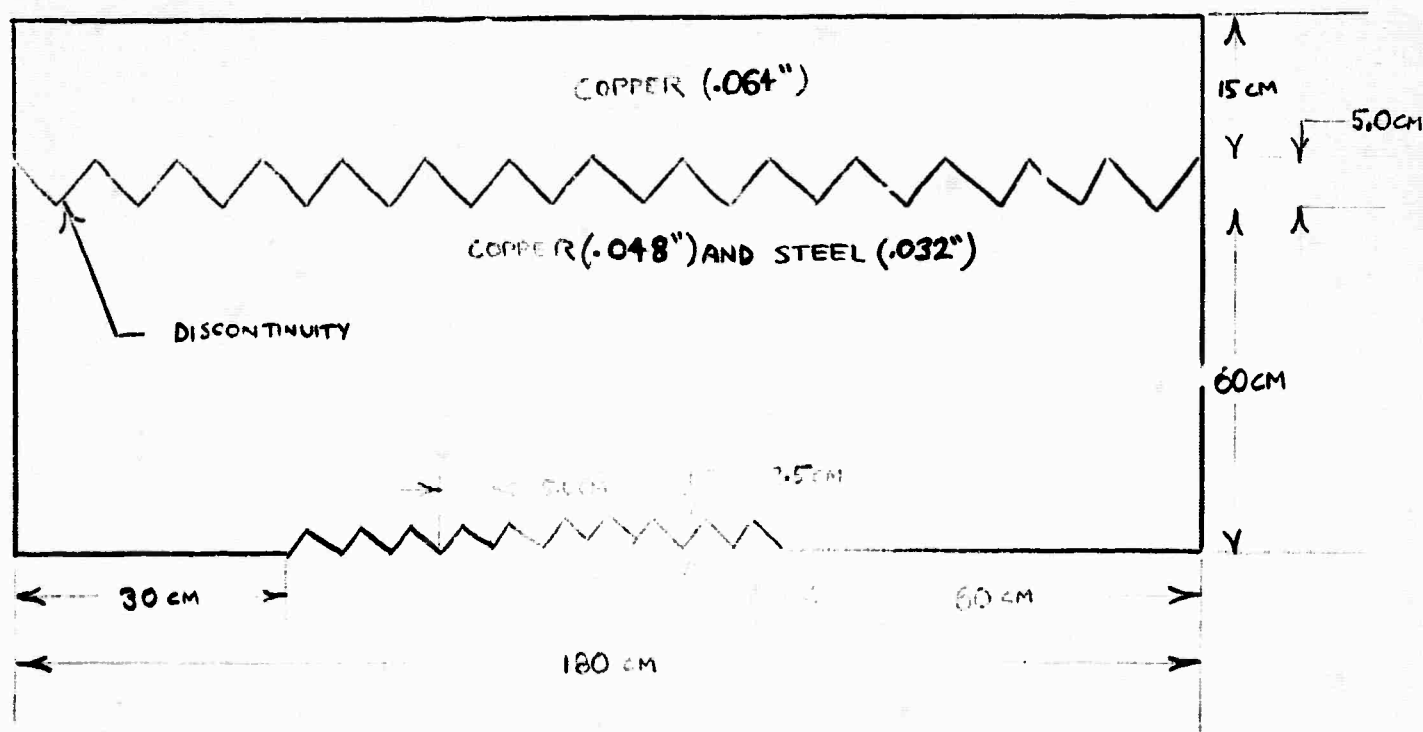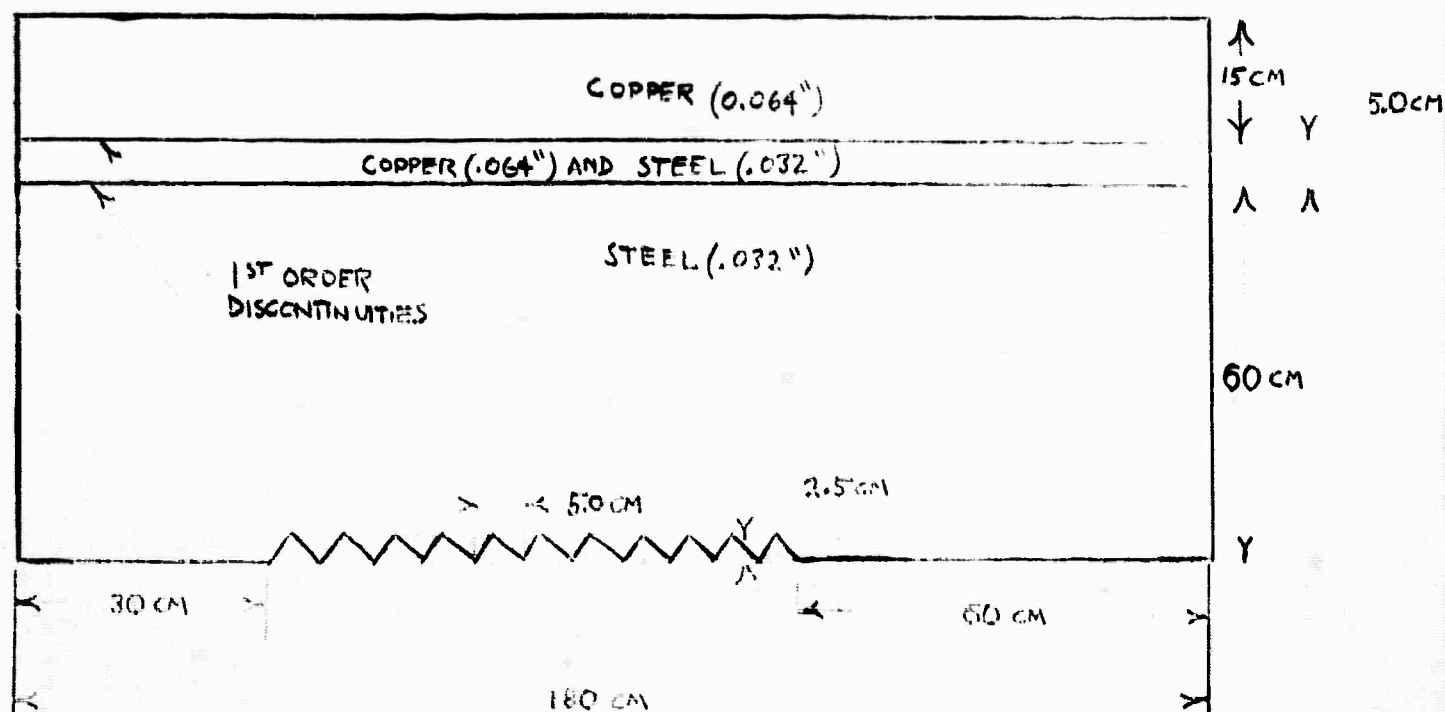
Figure 9. Average spectrum of all 37 stations

Figure 10.   The two models being tested